IJNRD.ORG ISSN : 2456-4184
INTERNATIONAL JOURNAL OF NOVEL RESEARCH AND DEVELOPMENT (IJNRD) | IJNRD.ORG
An International Open Access, Peer-reviewed, Refereed Journal

OPTIMIZED HIGH EFFICIENCY PV GRID INTEGRATION USING SWARM INTELLIGENCE-BASED PI CONTROLLER AND ADVANCED DC-DC CONVERTER

[1]Asif Iqubal, [2]Ashraf Ali, [3]MD Shoaib Akhtar, [4]Dr. B. Kavya Santhoshi

[1]UG Student, [2] UG Student, [3] UG Student, [4] Assistant Professor
[1,2,3,4] Department of Electrical and Electronics Engineering,
[1,2,3,4] Godavari Institute of Engineering and Technology (Autonomous), Rajahmundry, A.P., India.

Abstract: The rising demand for renewable energy has increased interest in photovoltaic (PV) systems as a sustainable alternative to fossil. The growing demand for renewable energy has driven advancements in photovoltaic (PV) technology. As solar energy becomes more widespread, integrating PV systems into the electrical grid efficiently is crucial for maintaining stability, reliability, and optimal performance. A key challenge in this integration is managing the variability and intermittency of solar power. This project proposes a high-efficiency PV grid integration system using a swarm intelligence-optimized PI controller and an enhanced DC-DC converter. The system begins with electricity generation from the PV panels, which is then stepped up in voltage by an enhanced Cuk-Boost converter. The output is processed through an isolated fly back converter to ensure stability and isolation. A PWM generator controls the converter's switching, and a Chaotic Rat Swarm Optimized PI controller regulates the DC voltage. A reduced switch 31-level Cascaded H-Bridge Multilevel Inverter (CHB MLI) converts the DC into AC for grid connection, followed by an LC filter for smooth output. The system is implemented using Matlab 2021a, offering efficiency and grid compatibility.

Index Terms **– Renewable Energy, Grid Integration, High-Efficiency PV System, PI Controller, Cuk-Boost Converter**

I. INTRODUCTION

The global transition to renewable energy has made the integration of photovoltaic (PV) systems into the electrical grid a crucial aspect of modern energy infrastructure. PV systems provide a sustainable alternative to fossil fuels by converting sunlight into electricity using semiconductor technology [1]. However, integrating these systems poses challenges, particularly the intermittent nature of solar energy. Unlike traditional power plants that produce electricity consistently, solar power generation fluctuates with weather conditions and daylight, leading to potential grid instability in terms of voltage and frequency.

To address these challenges, grid-tied inverters are used to convert the DC output from PV panels into AC for grid compatibility. Additionally, energy storage technologies, such as batteries, store excess solar power during peak sunlight hours and release it during low output or high demand, improving grid reliability. Demand-side management and load-shifting strategies optimize energy consumption by aligning usage with periods of high solar generation. Smart grid technologies are also essential for PV grid integration [2-5]. These systems enable real-time monitoring and control of electricity flow through digital communication, enhancing grid efficiency and flexibility.

Advanced forecasting methods improve the accuracy of solar power predictions, aiding in better energy dispatch planning [15].As PV systems become more widespread, grid congestion becomes a concern, particularly in regions with high solar penetration [6,7]. Addressing this requires significant upgrades to grid infrastructure and careful planning to avoid overloads and maintain stability. Regulatory frameworks, including clear technical standards for system interconnection and incentives for energy storage, are vital to support PV integration [8-10].

Successful PV grid integration reduces carbon emissions, enhances energy security, and contributes to a sustainable energy future [11,12]. With ongoing advancements in grid infrastructure, storage technologies, and PV systems, the role of solar energy in the global energy mix is expected to grow significantly in the coming years [13,14].

II. SYSTEM DESCRIPTION

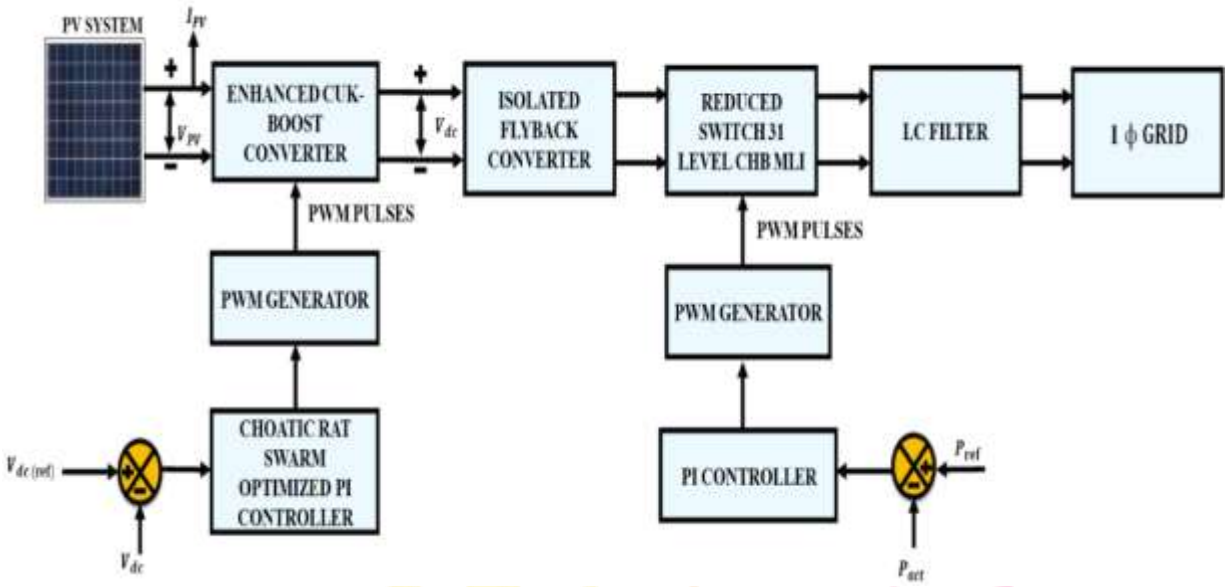

Figure 1. Block diagram of proposed system

This proposed system features high-efficiency PV grid integration using a swarm intelligence-optimized PI controller and an enhanced DC-DC converter. It begins with a photovoltaic (PV) system generating electricity, which is then stepped up in voltage using an enhanced Cuk-Boost converter. The output is processed through an isolated flyback converter for stability and isolation. A Pulse Width Modulation (PWM) generator controls the converter's operation, producing precise PWM pulses for efficient switching. The DC voltage is regulated by a Chaotic Rat Swarm Optimized PI Controller, ensuring optimal performance under varying conditions. To convert the DC output into a grid-compatible AC waveform, a reduced-switch 31-level Cascaded H-Bridge Multilevel Inverter (CHB MLI) is used. An LC filter smooths the output before feeding it into the single-phase grid. Designed for robustness and flexibility, this system enhances energy efficiency and grid compatibility, making it ideal for modern renewable energy applications.

A. PV System

Photovoltaic (PV) grid integration involves converting solar energy into electricity and supplying it to the electrical grid. Solar panels generate direct current (DC) electricity, which is then converted into alternating current (AC) by an inverter. The AC electricity is synchronized with the grid's voltage and frequency before being fed into the distribution network. Smart grid technologies optimize energy flow, ensuring real-time supply and demand balance. Energy management systems monitor and control the PV system's output for efficient dispatch. Grid integration also supports distributed generation, reducing transmission losses, and net metering policies encourage renewable energy adoption by crediting excess energy.

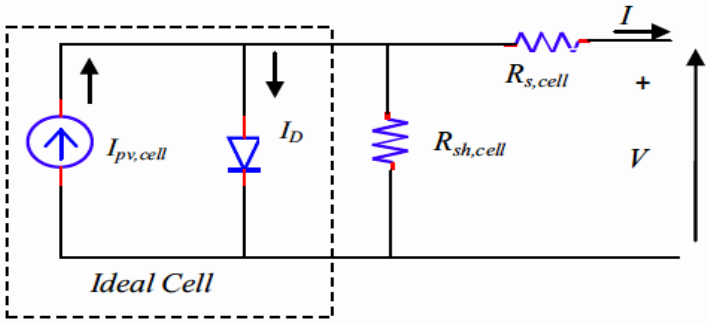

Figure 2. Circuit Diagram of PV system

B. Enhanced Cuck-Boost Converter

The enhanced Cuk-Boost converter is a combination of the boost and Cuk DC-to-DC converters, designed to achieve improved voltage gain, higher efficiency, and reduced stress. This hybrid converter takes advantage of the benefits of both the Cuk and boost converters. The system consists of a single switch (S), two inductors (L1 and L2), two diodes (D1 and D2), and three capacitors (C1, C2, and C3), each contributing to the converter's enhanced performance and efficiency.

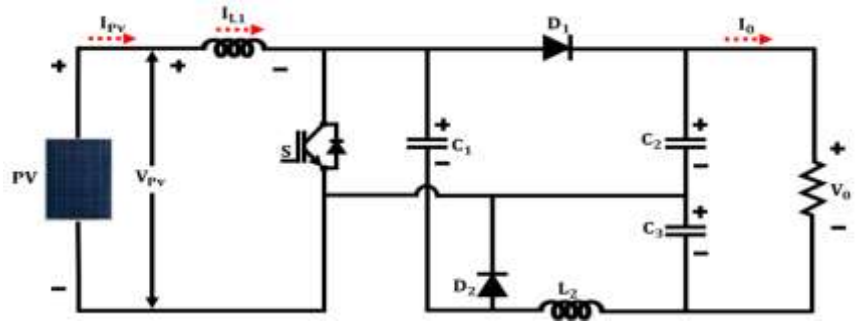

Figure 3. Enhanced Cuk-Boost Converter

The enhanced Cuk-Boost converter operates based on three distinct modes, which are explained as follows:

Mode 1: In this mode, the switch (S) is in the ON state, while diodes D1 and D2 are in the OFF (non-conducting) state due to the negative voltages across capacitors C1 and C2, respectively. During this phase, inductors L1 and L2 are in the charging state, and capacitor C1 is discharging, as illustrated in Figure 4. This mode ensures efficient energy transfer and voltage regulation.

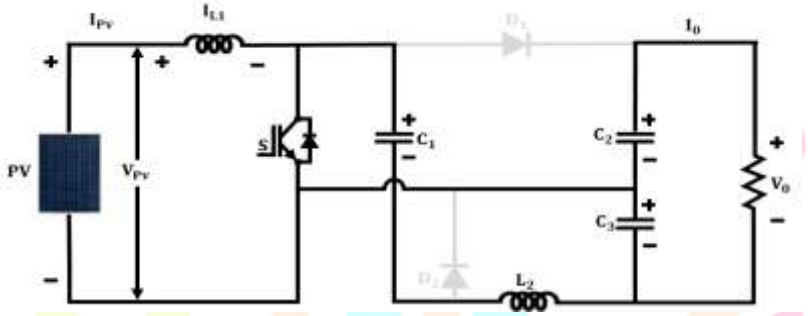

Figure 4. Mode 1 operation of enhanced Cuk-boost converter

Mode 2: In this mode, the switch (S) is in the OFF state, and diode D2 is also OFF, while diode D1 is turned ON. This causes the voltage across capacitor C1 to become less than the voltage across C2. As a result, the energy stored in inductors L1 and L2 decreases, as shown in Figure 5. This mode facilitates the energy transfer between components and contributes to the overall voltage regulation process.

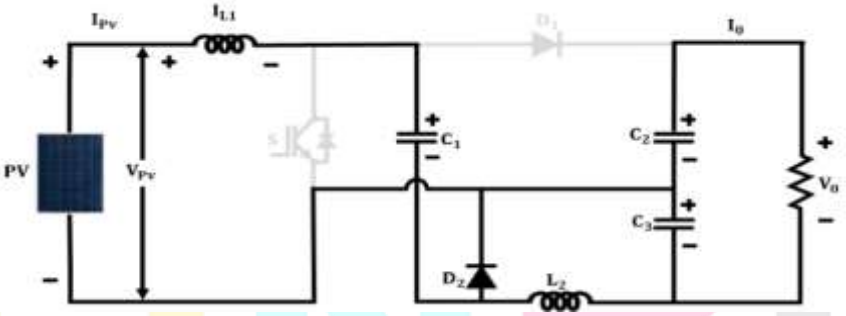

Figure 5. Mode 2 operation of enhanced Cuk-boost converter

Mode 3: In mode 3, Switch S is kept in OFF while both the diodes D_1 and D_2 are turned ON where V_{C2} is less or equal to V_{C1} and the inductors L_1 and L_2 gets discharged while capacitors C_1 , C_2 are charging which makes the current flow through L_1 as illusrated in figure 6.

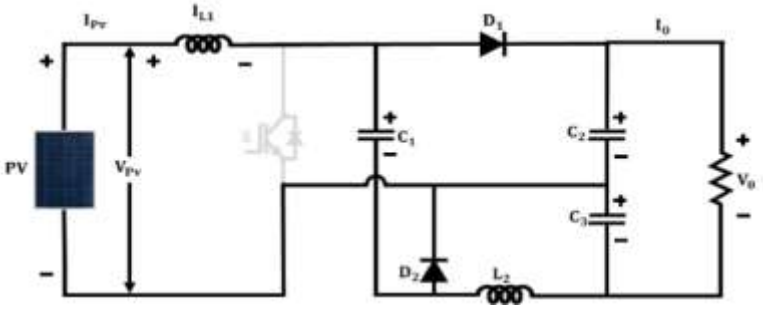

Figure 6. Mode 3 operation of enhanced Cuk-boost converter

In mode 3, Switch S is kept in OFF while both the diodes D_1 and D_2 are turned ON where V_{C2} is less or equal to V_{C1} and the inductors L_1 and L_2 gets discharged while capacitors C_1 , C_2 are charging which makes the current flow through L_1.

III. RESULTS AND DISCUSSIONS

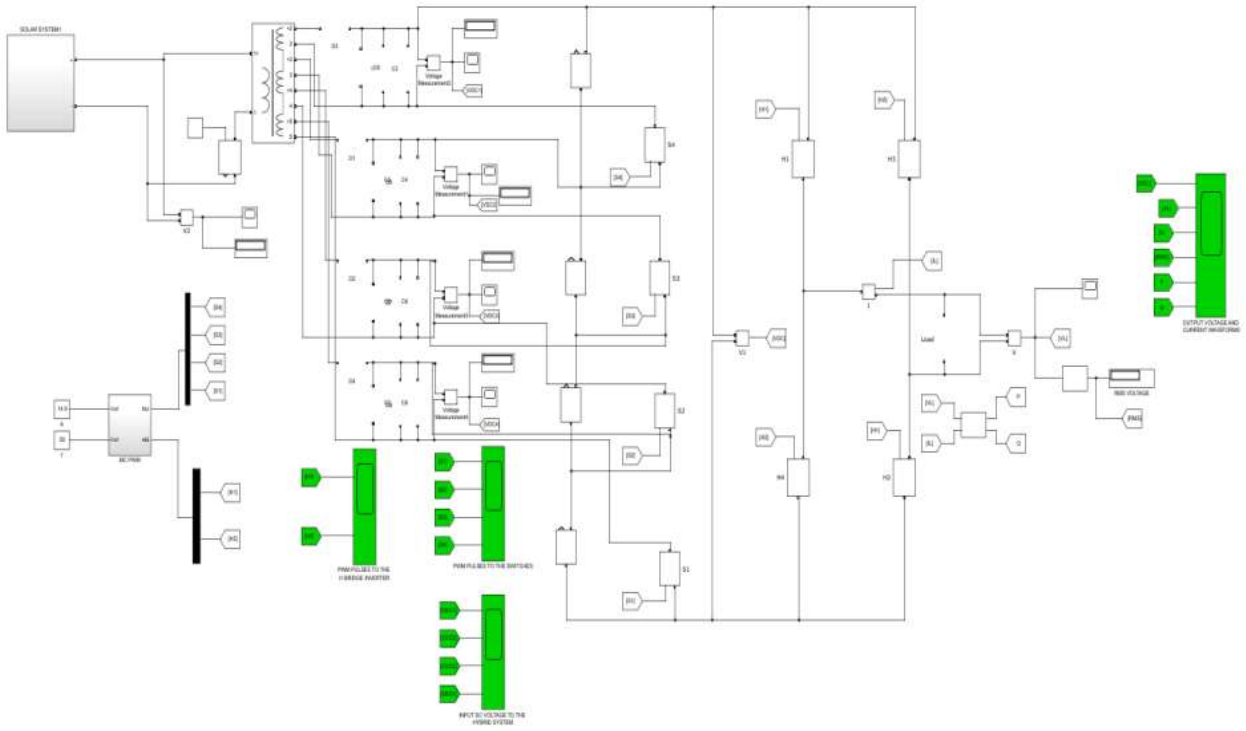

Figure 8. Overall Simulation

Figure 8 illustrates the comprehensive simulation diagram of the proposed work.

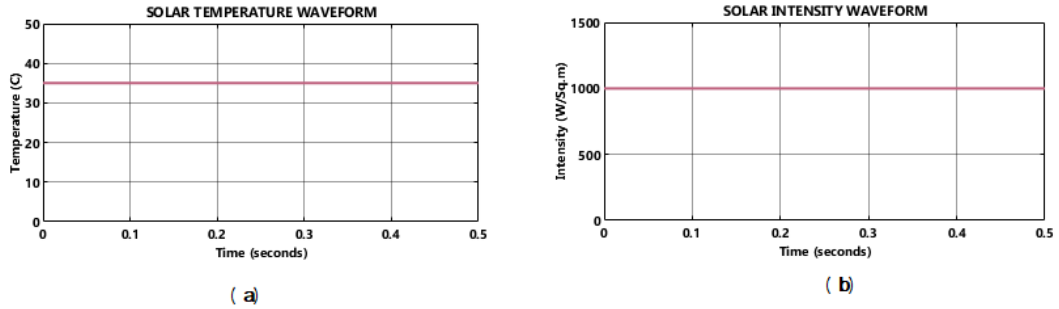

Figure 9. Solar temperature and intensity Waveform

Figure 9 illustrates the following waveforms: (a) solar temperature and (b) solar intensity. The temperature remains constant at 35°C throughout the observed time period, while the solar intensity stays steady at 1000 W/m², reflecting a consistent solar energy output.

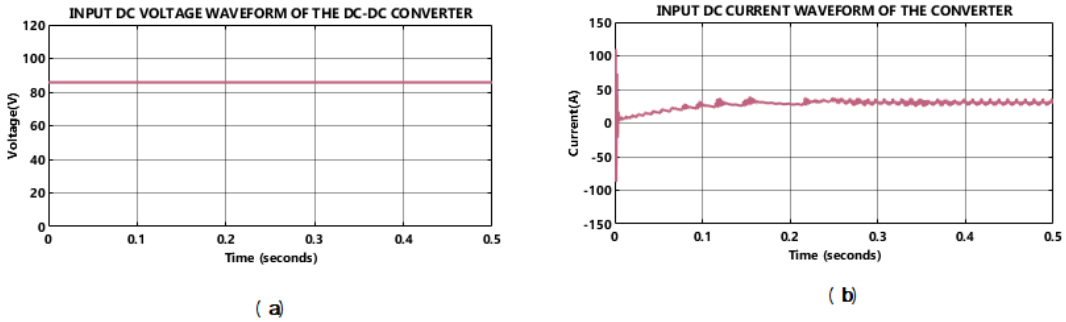

Figure 10. Input DC voltage and current waveform

Figure 10 depicts the input DC waveforms: (a) voltage and (b) current. The voltage remains stable at 85V over the 0.5-second interval, while the input current initially fluctuates but gradually increases to 40A. This behavior highlights the system's reliable and efficient performance.

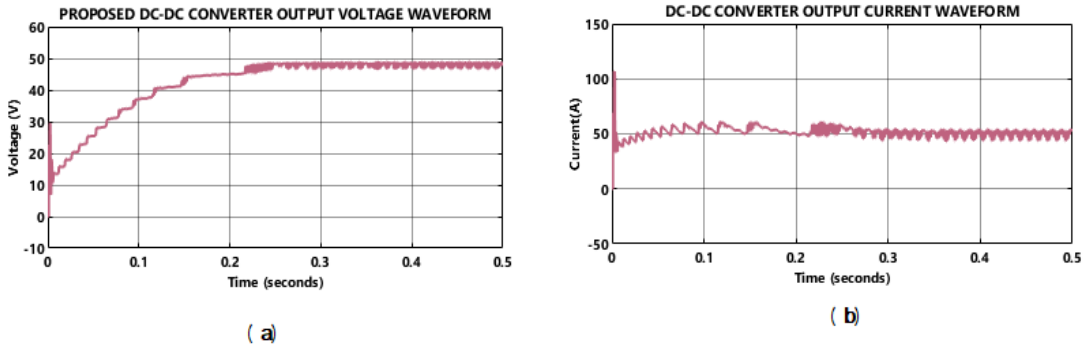

Figure 11. Output DC-DC Converter voltage and current waveform

Figure 10 illustrates the output waveforms of the DC-DC converter. In (a), the output voltage gradually increases and stabilizes at 49V after 0.2 seconds. In (b), the output current waveform initially fluctuates but eventually stabilizes at 50A.

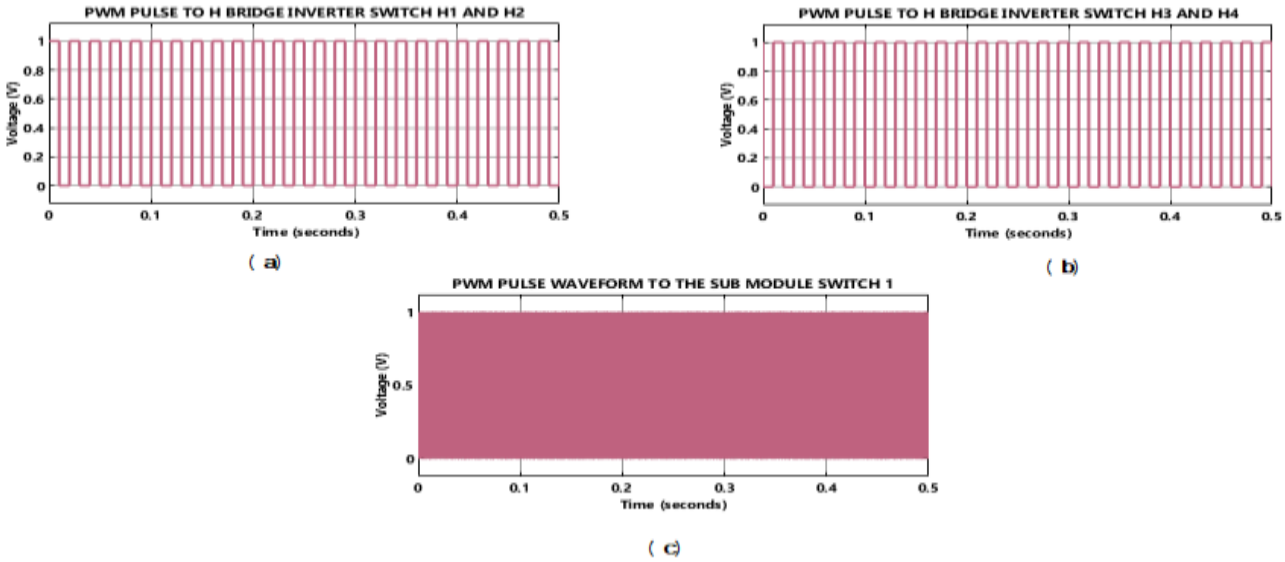

Figure 12. PWM pulses waveform

Figure 12 presents the PWM pulse waveforms. In (a) and (b), the pulses for H-bridge inverter switches (H1, H2) and (H3, H4) range between 0–1V. In (c), the PWM pulse for Submodule Switch 1 also fluctuates within the 0–1V range, demonstrating consistent voltage variation.

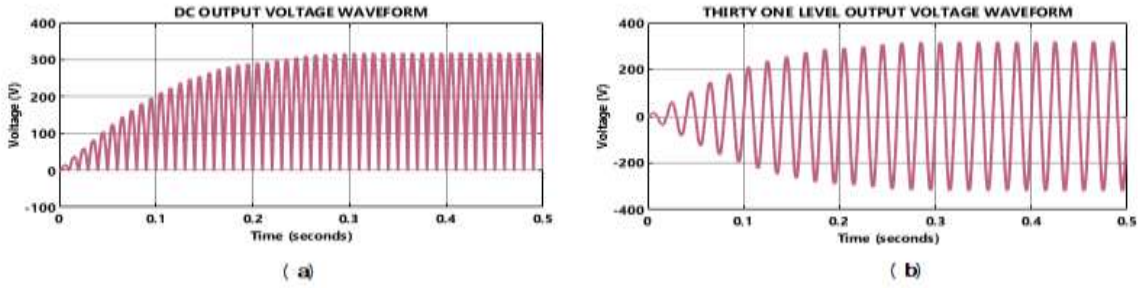

Figure 13. Output voltage of DC and Thirty one level waveform

Figure 13 illustrates output voltage waveforms. In (a), the DC output voltage gradually rises and stabilizes at 300V. In (b), the thirty-one-level output voltage steadily increases and stabilizes beyond ±200V.

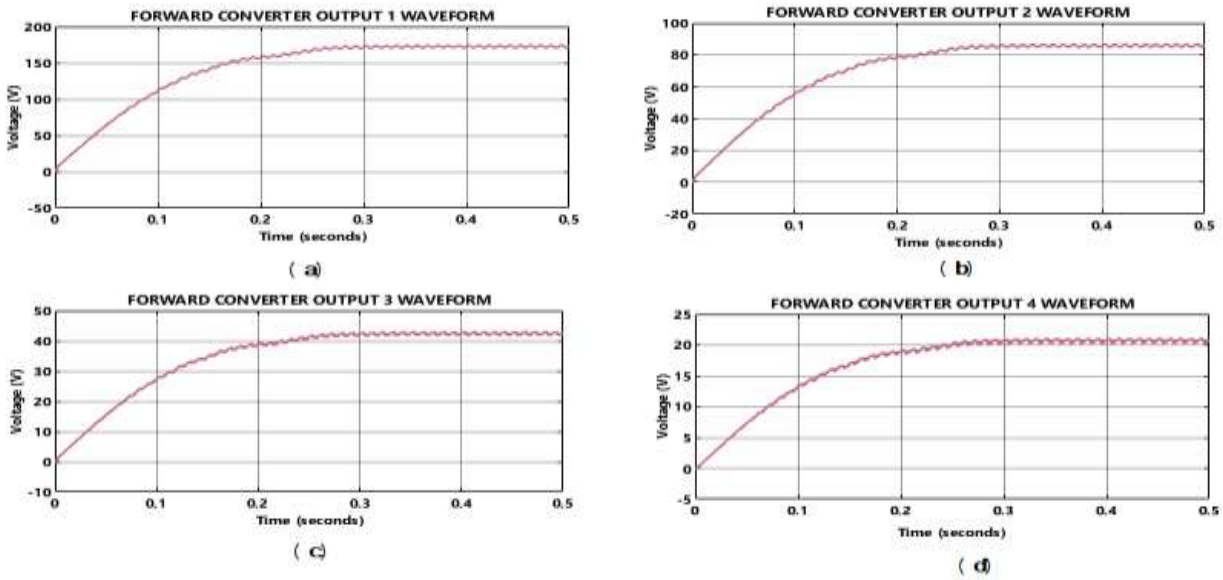

Figure 14. Forward converter output 1, 2, 3 and 4 waveform

Figure 14 presents the output waveforms of the forward converter. The first graph shows the output voltage gradually rising and stabilizing at 175V after 0.3 seconds. The second graph indicates a slight increase in voltage, stabilizing at 85V. The third and fourth graphs show stabilization at 42V and 20V, respectively, after 0.3 seconds.

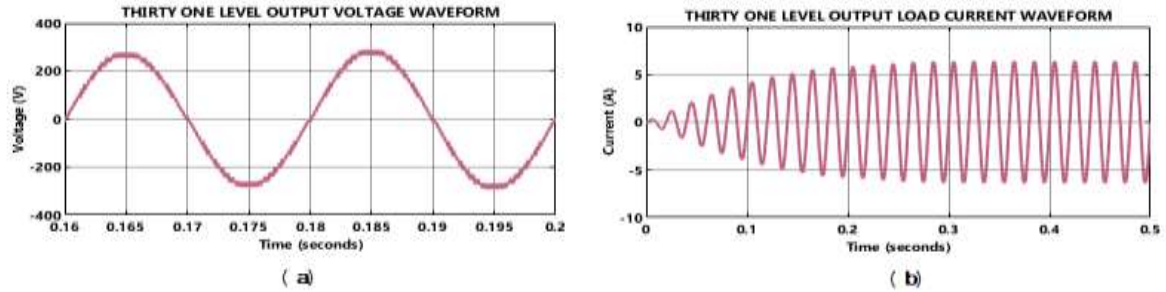

Figure 15. Thirty one level output voltage and current waveform

Figure 15 represents the performance of the thirty-one-level output. In (a), the sinusoidal voltage waveform peaks beyond ±200V, with its smoothness indicating reduced harmonic distortion. In (b), the output load current gradually increases and stabilizes after 0.2 seconds.

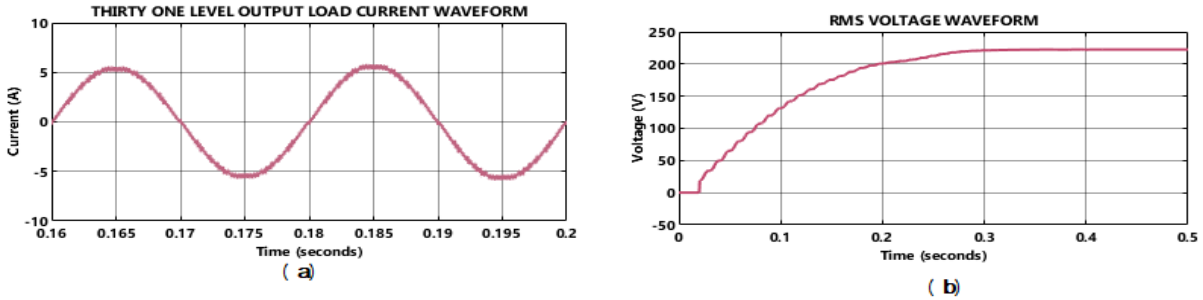

Figure 16. Waveform of thirty one level output and RMS voltage

Figure 16 shows the key waveforms of the thirty-one-level output. In (a), the sinusoidal current waveform peaks at 5A. In (b), the RMS voltage waveform gradually rises to 200V and stabilizes after 0.3 seconds for the remainder of the observed time period.

Figure 17 presents the real and reactive power waveforms. In (a), the real power steadily increases to 1000W and stabilizes after 0.3 seconds. In (b), the reactive power remains at 0, indicating improved power utilization.

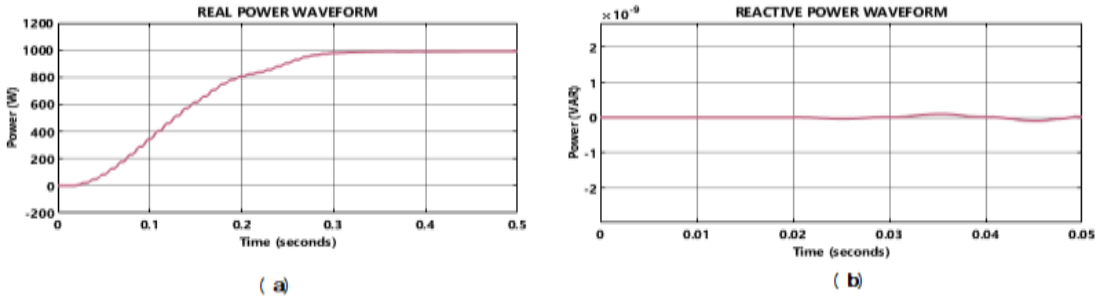

Figure 17. Real and Reactive power waveform

V. CONCLUSION

This paper develops a PV grid integration system featuring an enhanced Cuk-Boost converter and an optimized CRSO-based PI controller for highly efficient power conversion. Integrating photovoltaic (PV) energy into the grid generates clean power with minimal greenhouse gas emissions, promoting environmental sustainability. The enhanced Cuk-Boost converter improves output voltage stability, while the optimized CRSO-based PI controller ensures superior output quality and efficiency. The isolated Fly back converter contributes by delivering harmonic-free outputs with multiple voltage levels. The reduced-switch 31-level Cascaded H-Bridge Multilevel Inverter (CHB MLI) achieves multiple voltage levels with fewer switches, reducing Total Harmonic Distortion (THD) and enhancing system performance. Simulation results in MATLAB/Simulink demonstrate that the system achieves an impressive efficiency of 97%.

REFERENCES

1. Middelhauve, L., Terrier, C. and Marechal, F., 2022. Decomposition strategy for districts as renewable energy hubs. Ieee Open Access Journal of Power and Energy, 9, pp.287-297.
2. Akhtar, I., Jameel, M., Altamimi, A. and Kirmani, S., 2022. An innovative reliability oriented approach for restructured power system considering the impact of integrating electric vehicles and renewable energy resources. IEEE Access, 10, pp.52358-52376.
3. Albogamy, F.R., Paracha, M.Y.I., Hafeez, G., Khan, I., Murawwat, S., Rukh, G., Khan, S. and Khan, M.U.A., 2022. Real-time scheduling for optimal energy optimization in smart grid integrated with renewable energy sources. IEEE Access, 10, pp.35498-35520.
4. Patel, R.K., Kumari, A., Tanwar, S., Hong, W.C. and Sharma, R., 2022. AI-empowered recommender system for renewable energy harvesting in smart grid system. IEEE Access, 10, pp.24316-24326.
5. Jena, C., Guerrero, J.M., Abusorrah, A., Al-Turki, Y. and Khan, B., 2022. Multi-objective generation scheduling of hydro-thermal system incorporating energy storage with demand side management considering renewable energy uncertainties. IEEE Access, 10, pp.52343-52357.
6. Platero, G.G., Casado, M.G., García, M.P., Madero, P.J. and Baeza, D.A., 2022. CECRE: supervision and control of Spanish renewable energies in the last 15 years. Journal of Modern Power Systems and Clean Energy, 10(2), pp.269-276.
7. Bindu, A.A. and Thampatty, K.S., 2023. Optimal design and techno-socio-economic analysis of gird-connected hybrid renewable system. IEEE Access.
8. B. K. Santhoshi, K. M. Sundaram, A. Hussain, P. Sanjeevikumar, J. B. Holm-Nielsen, and V. K. Kaliappan, "Deep Learning for Fault Diagnostics in Bearings, Insulators, PV Panels, Power Lines, and Electric Vehicle Applications—The State-of-the-Art Approaches," in IEEE Access, vol. 9, pp. 41246-41260, 2021
9. Santhoshi, B.K., Mohanasundaram, K. & Kumar, L.A. ANN-based dynamic control and energy management of inverter and battery in a grid-tied hybrid renewable power system fed through switched Z-source converter. Electr Eng 103, 2285–2301 (2021). https://doi.org/10.1007/s00202-021-01231-7
10. Kavya Santhoshi, B.; Mohana Sundaram, K.; Padmanaban, S.; Holm-Nielsen, J.B.; K. K., P. Critical Review of PV Grid-Tied Inverters. Energies 2019, 12, 1921. https://doi.org/10.3390/en12101921
11. Ahmadifar, A., Ginocchi, M., Golla, M.S., Ponci, F. and Monti, A., 2023. Development of an energy management system for a renewable energy community and performance analysis via global sensitivity analysis. IEEE Access, 11, pp.4131-4154.
12. Giglio, E., Novo, R., Mattiazzo, G. and Fioriti, D., 2023. Reserve provision in the optimal planning of off-grid power systems: impact of storage and renewable energy. IEEE Access.
13. Wu, Q.H., Bose, A., Singh, C., Chow, J.H., Mu, G., Sun, Y., Liu, Z., Li, Z. and Liu, Y., 2023. Control and stability of large-scale power system with highly distributed renewable energy generation: viewpoints from six aspects. CSEE Journal of Power and Energy Systems, 9(1), pp.8-14.
14. Lin, C.H., Khan, M.S., Ahmad, J., Liu, H.D. and Hsiao, T.C., 2024. Design and analysis of novel high-gain boost converter for renewable energy systems (RES). IEEE Access.
15. Phophongviwat, T., Boonlert, T. and Hongesombut, K., 2024. Enhancing Grid Stability Using a Virtual Inertia-Integrated Railway Power Conditioner in Railway Power Supplies With High Renewable Energy Penetration. IEEE Access.